Shifts in mutation spectra enhance access to beneficial mutations

Mrudula Sane[1], Gaurav D Diwan[1,2,3], Bhoomika A Bhat[1,4], Lindi M Wahl[5]* and Deepa Agashe[1]*

[1] National Centre for Biological Sciences, GKVK Campus, Bellary Road, Bengaluru, India

[2] CellNetworks, Bioquant, University of Heidelberg, 69120 Heidelberg, Germany

[3] Biochemie Zentrum Heidelberg (BZH), University of Heidelberg, 69120 Heidelberg, Germany

[4] Undergraduate Programme, Indian Institute of Science, Bengaluru, India

[5] Western University, London, Ontario, Canada

*Correspondence to:

dagashe@ncbs.res.in

lwahl@uwo.ca

ABSTRACT

Biased mutation spectra are pervasive, with widely varying direction and magnitude of mutational biases that influence genome evolution and adaptation. Why are unbiased spectra rare, and how do such diverse biases evolve? Our experiments show that changing the mutation spectrum allows populations to sample previously under-sampled mutational space, including beneficial mutations. The resulting shift in the distribution of fitness effects is advantageous: beneficial mutation supply and beneficial pleiotropy both increase, and deleterious load reduces. More broadly, simulations indicate that the evolution of a mutational bias in an unbiased ancestor is selectively neutral; but reversing the direction of a long-term bias is always selectively favoured. Indeed, we predict frequent spectrum changes in the bacterial phylogeny, typically involving reversals of ancestral bias. Thus, shifts in mutation spectra may evolve under selection, and can directly alter the outcome of adaptive evolution by facilitating access to beneficial mutations.

SIGNIFICANCE STATEMENT

Mutations are important because they provide raw material for evolution. Some types of mutations occur more often than others, but the direction and degree of such mutational biases varies. How do mutational biases evolve, and do they influence evolution? We experimentally measured the immediate effects of changing the mutation bias of *E. coli*, and used simulations to test the long-term effects. Altering mutational bias is beneficial whenever the new bias increases sampling of mutational classes that were previously under-sampled. We also show that historically, bacteria have often experienced such beneficial bias switches. Our work demonstrates the importance of mutational biases in evolution. By allowing exploration of new mutational space, altered mutation biases could drive rapid adaptation even in constant environments.

INTRODUCTION

The mutation spectrum describes the frequency of various classes of sampled mutations (e.g., transversions vs. transitions (Tv/Ts)), and is often determined by the action of DNA repair enzymes. By determining the pool of genetic variants available for selection, mutation spectra can shape key genome features (e.g., nucleotide (1, 2), codon and amino acid composition (3)), even under selection for thousands of generations (4); determine the genetic basis of adaptation (5–9), driving convergent evolution (10–12); and shape the evolution of resistance to antibiotics (13–15) and anti-cancer drugs (16). Thus, mutation spectra are important for adaptive evolution, but their role is underappreciated (5). The mutation spectrum is instantaneously and relatively easily altered by loss-of-function mutations in DNA repair genes, e.g., as observed in “mutators” that also have higher mutation rates (17). The elevated mutation rate increases the supply of beneficial mutations, facilitating rapid adaptation (18). However, spectrum shifts also occur without associated mutation rate changes, such as with the loss of some bacterial DNA repair enzymes (17), and under nutritional or anaerobic stress (19, 20). Diverse mutation spectra occur even across natural yeast strains and closely related species of *Chlamydomonas*, despite similar mutation rates (21, 22).

In fact, most species analysed so far have a skewed mutation spectrum (i.e., some mutational classes are over-represented relative to the null expectation), with substantial variation in the direction and magnitude of bias (23, 24) (experimental data from microbes summarized in Table S1). This diversity implies major evolutionary shifts in mutation spectra. However, the frequency, underlying evolutionary processes, and consequences of spectrum shifts are unknown. For instance, why are unbiased spectra rare? Do spectrum shifts – for example, a change from an unbiased to a biased state, or altered direction of bias – evolve under selection? A spectrum shift may persist if the new bias favours mutational classes that are inherently advantageous (5, 25), allowing the evolved bias to hitchhike with beneficial mutations. It has also been speculated that stress-induced changes in mutation spectra may enhance sampling of new beneficial mutations by altering the distribution of fitness effects (DFE) (19, 26). However, prior studies have failed to find consistent support for general selective benefits of specific mutational classes. For instance,

transition mutations (Ts) are not consistently more beneficial (or less deleterious) than transversions (Tv) (27, 28); and the fixation probability of Ts vs. Tv mutations in genomes is clade-specific (29). Hence, particular mutational classes do not seem to be universally beneficial, and the observed diversity in mutation bias remains puzzling.

We addressed these gaps using a combination of experiments, simulations, and phylogenetic analyses. To measure the immediate evolutionary impact of the mutation spectrum, we estimated the genome-wide DFE of new mutations in *Escherichia coli*. We manipulated the mutation spectrum by deleting a DNA repair gene (Δ*mutY*, "mutator" strain) from our wild type strain ("WT"), altering both the mutation spectrum and rate (17). Allowing independent lineages of both strains to evolve under mutation accumulation (MA), we sequenced whole genomes of evolved isolates to identify strains carrying a single new mutation each. Thus, we minimized the impact of selection on the mutation spectrum and the DFE, while also decoupling the effects of the mutator's spectrum from its high mutation rate. Measuring the effect of each single mutation on population growth rate, we determined the effects of mutation spectrum on the beneficial mutation supply, genetic load, and pleiotropic effects. Next, to test the generality and longer-term evolutionary consequences of shifts in mutation spectra, we performed both adaptive walk and full population simulations. Finally, we inferred evolutionary transitions in DNA repair enzymes across the bacterial phylogeny to estimate the frequency of shifts in mutation bias. Our results show that shifts in mutation spectra can evolve under selection and fuel adaptation via previously under-sampled evolutionary paths.

RESULTS AND DISCUSSION

The mutator DFE has more beneficial mutations that reduce the expected genetic load and alter pleiotropic effects

From MA experiments conducted in rich media (LB), we obtained 80 evolved WT (30) and 79 mutator strains, each carrying a single distinct mutation with respect to its ancestor (Supplementary Data). We measured the selective fitness effect (relative growth rate) of each mutation in the MA

environment (LB) as well as 15 other environments with different carbon sources, including some that are used by *E. coli* in the mouse gut (31). With this large set of fitness effects, we constructed environment-specific empirical DFEs (WT data for some environments were previously reported (30)). Since bacterial MA experiments can cause over-sampling of beneficial mutations and under-sampling of deleterious mutations, we used a correction (32) that retains the measured selective effect (s) of each mutation, but estimates and corrects for selection bias by changing the frequency of mutations with a given selective effect (Fig. S1A–C, Supplementary Data). These corrected DFEs thus provide accurate estimates of the fraction of beneficial mutations (f_b) and the average selective effect (s).

Correcting for selection bias during MA results in DFEs with coarsely binned fitness histograms, we calculated the fraction of neutral ($-0.05 < s < 0.05$, conservatively accounting for a maximum of ~5% fitness measurement error), beneficial ($s > 0.05$), and deleterious ($s < -0.05$) mutations for each strain in all 16 environments. The DFEs and f_b values varied across environments (Fig. 1, Fig. S1), but on average the mutator had a greater fraction of beneficial mutations (f_b = 36% vs. 28%) and fewer deleterious mutations (Fig. 1, Table S2). Thus, compared to WT, the mutator had more beneficial-shifted DFEs. Mean fitness effects of mutations were also significantly more beneficial in the mutator (paired Welch's two-sample test, $p = 0.043$; Fig. S2A), although medians were not significantly different ($p = 0.35$, Fig. S2B). Finally, mutations had larger absolute effects in WT than in the mutator (Wilcoxon's rank-sum test, $W = 662920$, $p = 1.4\times10^{-14}$); hence, the mutator's beneficial-shifted DFEs could not have arisen because of overall larger-effect mutations. These results indicate a broad selective advantage to the mutator, independent of its mutation rate. In addition, accounting for the skewed DFEs and order-of-magnitude higher mutation rate ($\mu_{WT} = 9.3\times10^{-11}$ per bp per generation, $\mu_{mutator} = 89\times10^{-11}$, Table S3), we estimated (following (33)) that on average the mutator should have an ~16-fold greater genome-wide supply of beneficial mutations, and ~6-fold higher genetic load than the WT (Tables S4, S5). In contrast, if we ignored the mutator's distinct DFE and accounted only for its mutation rate, both the supply of beneficial mutations and the deleterious genetic load would be nearly 10-fold greater than WT (Tables S4, S5; only the load is significantly affected by the correct DFE). Thus, depending on their mutation

124 rate and DFE, mutators may have a substantially higher supply of beneficial mutations and smaller
125 genetic load than previously believed.
126
127 The high f_b values observed in some environments (Fig. 1) contradict the general expectation that
128 beneficial mutations should be rare (34). However, many other studies – including with microbes
129 and plants – have also reported a large number of beneficial mutations (35–41). Such large f_b
130 values have been partially attributed to an improved ability to measure small-effect beneficial
131 mutations (38, 42, 43) that are more common than expected (44), especially at low effective
132 population sizes (40). Most prior studies (34) provide approximate or indirect estimates of the DFE
133 via random mutagenesis of a single gene, and focus only on the beneficial part of the DFE, or infer
134 the DFE by fitting a model to time series data from selection or MA lines. Further, they do not
135 estimate the number of underlying mutations to account for epistasis. Our direct, genome-wide
136 estimates of the DFE of single, randomly-sampled new mutations support the idea (45, 46) that
137 new beneficial mutations may be more common than generally believed.
138
139 Next, we estimated the pleiotropic effects of mutations (Fig. 2A), which are important because they
140 can facilitate adaptation (via synergistic pleiotropic benefits) and shape fitness tradeoffs (via
141 antagonistic pleiotropy) in new environments. The mutator had a distinct distribution of pleiotropic
142 effects in all 16 environments (compare Fig. S2C–D, chi-square tests: $p < 10^{-5}$ in each case, Table
143 S6), driven by a higher incidence of beneficial synergistic pleiotropy and lower deleterious
144 synergistic pleiotropy. However, both strains had low antagonistic pleiotropy (Fig. 2B–C).
145 Beneficial mutations in the mutator were also beneficial across many more environments
146 (Kolmogorov-Smirnov test comparing the two distributions in Fig. 2F, $D=0.41$, $p=3.1\times10^{-6}$);
147 whereas deleterious mutations were deleterious in fewer environments than WT ($D=0.56$,
148 $p=2.63\times10^{-11}$; Fig. 2F, Fig. S3). Despite this qualitative association between mutational effects,
149 overall, the magnitude of fitness effects was not correlated across environments (only 38 of 120
150 correlations were significant in WT and 22 of 120 significant in mutator, Spearman's rank
151 correlation, $p < 0.05$). Thus, new beneficial mutations in the mutator are more likely to facilitate
152 adaptation across many environments, but are no more likely to generate tradeoffs. Interestingly,

153 simulating an increase in the median fitness effect of the WT DFE without changing its shape ("WT-
154 beneficial shift") mimicked pleiotropic effects observed in the mutator in all but two environments
155 (Fig. 2D, Fig. S2E, Table S6). Conversely, simply reducing the median fitness effect in the WT
156 DFE ("WT-deleterious shift") lowered beneficial synergistic pleiotropy in all 16 environments (Fig.
157 2E, Fig. S2F, Table S6). Ignoring the mutation spectrum can thus cause overestimation of a
158 mutator's genetic load, and underestimation of the supply and pleiotropic effects of beneficial
159 mutations.
160
161 **The mutator's beneficial-shifted DFEs arise from its distinct mutation spectrum**
162
163 We had hypothesized that the mutator's distinct DFE could arise from its biased spectrum.
164 However, other global effects of the initial *mutY* gene deletion could also lead to a DFE shift. For
165 instance, if deleting *mutY* reduced the mutator's fitness, a larger fraction of new mutations might
166 be beneficial (47). However, the mutator ancestor had lower fitness than WT in only three
167 environments (Fig. 3A, Table S7). Alternatively, epistatic interactions with *mutY* could increase the
168 deleterious effect of new mutations in the WT. However, paired WT and mutator strains carrying
169 the same mutation had similar fitness in all but one environment (Fig. 3B, Table S8). Thus, the
170 observed shift in the mutator DFE cannot be explained by global effects of the *mutY* deletion. The
171 difference across strains was also robust across mutational classes: mutations were more
172 beneficial in the mutator even when comparing only base-pair substitutions, or coding, non-coding,
173 synonymous, or non-synonymous mutations (Fig. S4).
174
175 Next, we asked whether the mutator is biased towards mutational classes that happen to be more
176 beneficial (or less deleterious). We defined mutation bias as the proportion of mutations belonging
177 to a specific mutational class (e.g., Tv bias = Number of Tv mutations / (Number of Tv + Number
178 of Ts mutations)). Note that the null expectation ("unbiased" state) differs across each type of bias.
179 For Tv bias, the null is 0.67 because 2/3rd of all possible single nucleotide changes are
180 transversions. For GC→AT bias, the null is 0.5 because for a randomly generated genome half of
181 all mutations should be GC→AT. For actual genomes with extreme GC content, the null

182 expectation will change (e.g., in a GC-rich genome, the baseline probability of AT→GC mutations
183 is less than 0.5 because there are few A or T bases that can mutate). This is not a major problem
184 for *E. coli* since its genomic GC content is ~50%. Regardless of the type of bias, we could compare
185 mutation biases across the new mutations sampled by WT and mutator, because barring the
186 deletion of *mutY* both ancestral genomes were identical. The mutator strongly favours
187 transversions, GC→AT mutations, base pair substitutions (BPS) and coding mutations (Fig. 3C,
188 Table S3). Overall, transversions and GC→AT mutations were less deleterious than transitions
189 and AT→GC mutations respectively (Fig. 3D–E; fitness effects pooled across environments, Table
190 S9), but the other mutation biases did not show consistent differences (Fig. S4, Table S9).
191 Additionally, other aspects of the mutations (e.g., genomic location or specific amino acid changes)
192 also did not differ across strains (Fig. S5, S6; Tables S10, S11). Thus, as predicted, the mutation
193 spectrum – specifically the strong Tv and GC→AT bias – appeared to drive the distinct DFE of the
194 mutator, because the mutator over-samples these specific mutational classes. However, it was
195 unclear why Tv and GC→AT mutations should be more beneficial.
196
197 **Simulations demonstrate a general benefit of reversing mutation spectra**
198
199 To test the generality of our empirical results and uncover underlying mechanisms, we simulated
200 adaptive walks in an NK fitness landscape ((48), see Methods), modelling sequences of N
201 nucleotides such that mutations could be classified as Ts vs. Tv or GC→AT vs. AT→GC. Starting
202 from a randomly chosen ancestor sequence and mutation spectrum (Tv bias = fraction of
203 transversions), we allowed populations to explore successive mutational steps at randomly chosen
204 loci (bases). A mutation that confers a relative fitness increase of 1+s fixes (a step in the walk is
205 taken) with probability 2s; that is, we assumed a strong-selection weak-mutation (SSWM) regime.
206 At various points during the walk, we simulated mutations to generate a DFE, computed fitness
207 effects given the underlying fitness landscape (affected by K other randomly chosen loci, to
208 incorporate epistasis), and calculated the fraction of beneficial (f_b) and deleterious (f_d) mutations
209 and their effect sizes. We initially set N=200 and K=1 (each locus epistatically coupled to

1/199=0.5% loci), and present the average outcomes for 500 adaptive walks on 500 randomly-generated fitness landscapes (Fig. S7A–B shows variation across walks).

As expected, mean population fitness increased during the adaptive walk, with a concomitant reduction in f_b and beneficial effect size, an increase in f_d, and a relatively constant deleterious effect size (Fig. 4A). Setting ancestral Tv bias to 0.45 (mimicking our WT), we compared the DFE generated by the ancestor at various time points, to the DFE that would be created if the bias were changed at that time point (mimicking our Δ*mutY* strain). The bias-shifted ("shifted") strain thus has the same fitness and sequence as the ancestor and an identical mutation rate, differing only in spectrum. As the ancestor evolved (i.e., f_b decreased), a stronger bias shift (i.e., higher Tv) allowed the bias-shifted strain to sample proportionally more beneficial mutations than the ancestor (Fig. 4B). More generally, exploring well-adapted populations (f_b = 0.04) but varying both the ancestral and shifted mutation spectra, we find that shifted strains that reverse the ancestral bias (i.e., have a strong bias in the opposite direction) have the greatest advantage (Fig. S8). Our results hold across a different axis of the mutation spectrum (GC→AT bias, Fig. S9), and in more rugged fitness landscapes with higher epistasis (Fig. S10A–B). Importantly, adapting populations did not "exhaust" a small set of beneficial mutations; rather, they fixed distinct mutations as they explored a large number of diverse pathways that represent a subset of many possible fitness peaks (Fig. S10C). Our results also hold in full population simulations with multiple segregating mutations (relaxing the SSWM assumption), where deleterious mutations can fix (Fig. 4C–D, Fig. S11). In fact, when more mutations are accessible, we observe the same beneficial effects of bias reversals, but these effects emerge more quickly. Finally**,** these effects are also observed in full population simulations when the fitness landscape is defined using a codon-based rather than a nucleotide model (Fig. S12).

Thus, our simulation results can be broadly generalized in the form of three key predictions: (1) reversing an ancestral mutation bias is always beneficial (2) the magnitude of the benefit increases with the degree to which the new bias opposes the ancestral bias, and (3) the magnitude of the benefit increases when the ancestor has evolved with a given bias for longer intervals of time (i.e.,

239 as the ancestor gets better-adapted over time). Our experimental data with the Δ*mutY* strain
240 support the first prediction, since we found that overall the mutator (with a reversal of the Tv bias,
241 Fig. 3D) had higher f_b values than WT. Interestingly, the WT GC→AT bias was reinforced in the
242 mutator, rendering the results in Fig. 3E puzzling. However, ~88% of all GC→AT mutations in the
243 mutator are also transversions. Hence, our mutator's observed beneficial-shifted DFE is explained
244 by its strong Tv bias, which opposes the existing WT bias towards Ts.
245
246 Although our data are generally explained by the simulation results, some puzzling observations
247 remain. The simulations predict that the mutator should have higher f_b in all environments, but we
248 do not observe this pattern as consistently as expected (Fig. 1). Further, in apparent contradiction
249 to prediction 3 above, the difference in f_b between WT and mutator in lowest in LB (where ancestral
250 growth rate is highest and presumably *E. coli* is best-adapted). However, note that our strains
251 evolved for a very short time in LB under minimal selection, so LB is not an "ancestral" environment
252 in an evolutionarily meaningful sense. Additionally, absolute growth rate is not a reliable indicator
253 of the relative degree of or period of adaptation to an environment, because it is also strongly
254 influenced by nutrient availability. Indeed, f_b was not correlated with ancestral growth rate across
255 environments in either strain (Spearman's rank correlation test, WT: rho = –0.217, Mutator: rho =
256 –0.18; $p > 0.05$ in each case). Hence, to understand the environment-specific differences in DFEs,
257 we need to explicitly test predictions 2 and 3 (described above) under conditions where the precise
258 degree of bias change and the length of evolutionary time in an environment can be measured
259 and/or manipulated.
260
261 Our simulation results demonstrate general conditions under which a change in mutational bias
262 can be selectively advantageous. But how does mutation bias evolve in the first place? Starting
263 from an unbiased ancestor, we find that introducing any bias is selectively neutral, regardless of
264 how long the ancestor had evolved in the same fitness landscape (Fig. 4E–F). However, if the
265 ancestor had previously evolved with a biased spectrum (e.g., our WT), the population would have
266 already sampled many beneficial mutations within the class favoured by the existing bias. Hence,
267 a shift in the opposite direction (e.g., in our Δ*mutY* strain) allows the population to explore

268 mutational space that was previously under-sampled, increasing the probability of finding new
269 beneficial mutations. Importantly, this means that the benefit of a specific mutation class (e.g., Tv)
270 is not universal, but is context-dependent. Increased sampling of any mutational class that was
271 previously poorly explored would therefore be beneficial. Thus, after a period of evolving with a
272 new spectrum, a change in the fitness landscape (e.g., due to epistasis or environmental change)
273 may again render a spectrum shift advantageous. Together, these results generate two additional,
274 broad predictions: (a) starting from an unbiased spectrum, a biased spectrum can only evolve
275 through drift, and (b) after a period of adaptation with a specific mutation bias (and/or following
276 environmental change), reversing the bias becomes beneficial. We tested the second prediction
277 using a broad phylogenetic analysis of bacterial taxa, expecting that evolutionary shifts in mutation
278 spectra should be enriched in bias reversals.
279
280 **Evolutionary transitions in DNA repair enzymes indicate mutation spectrum reversals in**
281 **most bacterial lineages**
282
283 Altering DNA repair function is a simple and instantaneous mechanism to generate spectrum shifts.
284 Hence, to infer long-term mutation spectrum dynamics we mapped evolutionary transitions in 11
285 bacterial DNA repair enzymes with empirically measured effects on mutation spectra, i.e., whose
286 loss changes the Tv or GC→AT bias in *E. coli* (Table S12). Identifying gene orthologues in 1093
287 extant bacterial genomes, we used ancestral reconstruction to infer enzyme gains and losses
288 across a pruned tree derived from a previously published whole-genome bacterial phylogeny
289 based on >400 proteins (following (49); Fig. 5A). Broadly consistent with previous work with a few
290 DNA repair genes (50), we found frequent evolutionary transitions in most repair enzymes with
291 known spectrum effects (Fig. 5A), as well as for 33 other genes with unknown effects on mutation
292 spectra (Fig. S13). Using the predicted set of enzymes present in each hypothetical ancestor
293 (nodes), we estimated the Tv and GC→AT bias at each node relative to WT *E. coli* and traced the
294 change in relative bias over time (Fig. 5B, Fig. S14A). Consistent with our simulation results,
295 successive enzyme gain or loss events led to a bias reversal in >80% lineages, and we observed
296 only a few cases of reinforced bias (Fig. 5C). This is distinct from the pattern expected by chance

297 (10,000 phylogenetic stochastic simulations using similar enzyme transition rates; Fig. 5C, Fig.
298 S14B). Notably, bias reversals are more frequent than expected (one-sample t-tests, Tv bias: t = -
299 72.38, $p<2x10^{-16}$; GC→AT bias: t = -59.42, $p<2x10^{-16}$) while reinforcements are less frequent than
300 expected (Tv bias: t = -72.38, $p<2x10^{-16}$; GC→AT bias: t = -59.42, $p<2x10^{-16}$) (Fig. S14C–D).
301 Hence, our results cannot be attributed to peculiarities of the enzyme set, tree topology, or number
302 of evolutionary transitions. Instead, we suggest that such frequent bias reversals likely reflect
303 selection on mutation rate and/or spectrum. Although it is difficult to separate these effects, two
304 pieces of evidence suggest that the observed dynamics at least partly reflect selection for reversal
305 of mutation spectra. First, enzymes with a weak effect on mutation rate but a strong impact on
306 spectrum are also highly dynamic (e.g. *ung* and *mutM*; Table S12). Second, for enzymes with a
307 strong impact on both mutation rate and spectrum, either bias reversals or reinforcements would
308 change mutation rates. Hence, selection for mutation rate alone cannot explain the higher-than-
309 expected frequency of bias reversals that we observe.
310
311 We discuss here a few limitations of this analysis. First, reconstruction of ancestral character states
312 in phylogenetic datasets is not always accurate and does not account for uncertainty in the
313 underlying phylogeny (51). Second, the estimated biases do not account for other repair enzymes
314 whose effects on the mutation spectrum are unknown, or for variation in the impact of enzyme loss
315 or gain. We also likely underestimate the actual number of bias shifts because we could not include
316 cases where repair function may be altered without gene deletion (e.g., due to loss-of-function
317 point mutations). However, given the lack of relevant empirical data for most bacteria, the values
318 we report are our best estimates of the mutation biases of diverse bacteria relative to *E. coli*, and
319 quantify at least a proportion of the "true" changes in mutation spectra that have occurred across
320 lineages. Available experimental data also show that the qualitative effects of deleting a specific
321 DNA repair enzyme are largely consistent across species (Table S13), suggesting that the broad
322 trends observed here should be robust. Finally, recent work indicates similar dynamics of genes
323 involved in DNA repair in bacteria (52) and fungi (53). Thus, sustained shifts in mutation spectra
324 likely occur frequently, and their long-term impacts on the pool of genetic variants available for
325 selection deserve further investigation.

326

327 **CONCLUSIONS**

328

329 We show that pervasive mutational biases can evolve by genetic drift, whereas shifts in the
330 strength and direction of bias could evolve under selection. Thus, a species' evolutionary history
331 may be sufficient to explain the evolution of genomic bias (e.g., in base composition), without
332 invoking specific underlying mechanisms or selection favouring particular mutational classes.
333 Previous work showed that the transversion-biased mutators Δ*mutT* and Δ*mutY* have distinct DFEs
334 for antibiotic resistance compared to WT, but the effect was attributed to transversions being more
335 beneficial for the specific antibiotic target (13). However, by recasting the puzzle of mutational
336 biases as a problem of searching a vast and dynamic mutational space, our model allows broad
337 generalization across mutation spectra. We suggest that the rarity of species with unbiased
338 mutation spectra is not surprising, since shifts from unbiased to biased spectra may occur easily
339 and frequently via changes in DNA repair function and are unopposed by selection. Hence, a
340 biased spectrum should be the norm rather than the exception.

341

342 While it is well established that access to *more* mutations (through an increased mutation rate) is
343 advantageous (18), here we demonstrate that accessing *different* mutations can likewise provide
344 an advantage. Our results have important implications for the evolution of mutator genotypes, in
345 which shifts in mutation spectra and mutation rates are often (though not always) entangled.
346 Mutator dynamics are governed by the genetic load and supply of beneficial mutations (18, 33,
347 54). In a new environment (away from fitness optima), these parameters are primarily driven by
348 mutators' high mutation rate (55) – particularly under strong selection (56) – allowing them to
349 hitchhike with beneficial mutations (57). We show here that the genome-wide beneficial supply
350 rate is strongly influenced by the mutation spectrum across environments, and this effect is
351 strongest in well-adapted populations. Further, we predict that the advantage of a high mutation
352 rate should be enhanced if accompanied by a reversal of the ancestral spectrum, but diminished
353 otherwise. A recent simulation study also predicts that differences in the mutation spectrum of
354 mutators can change the magnitude of deleterious mutations; such differences can facilitate the

355 loss of mutators under selection (58). Thus, mutation rate and spectrum may jointly govern the
356 observed rise, persistence, and fall of mutators under selection (13, 33, 59). Such effects may
357 explain why mutators with relatively small increases in mutation rate are also abundant in natural
358 bacterial populations (60), and deserve further attention (13, 58) with theoretical and experimental
359 analyses to dissect the role of mutation rate vs. spectrum.
360
361 Together with studies showing that mutation biases are pervasive and influence the genetic basis
362 of adaptation under diverse conditions (see Introduction), our results demonstrate that mutation
363 spectra may be important drivers of adaptation and innovation under myriad scenarios. When the
364 beneficial mutation supply is limited by the existing spectrum, an antiparallel (opposite direction on
365 the same axis) or orthogonal jump (on a different axis of the spectrum) could enhance sampling of
366 new beneficial mutations, facilitating rapid adaptation. Our phylogenetic analysis likely
367 underestimated such evolutionary shifts in mutation spectra, which may occur even more
368 frequently on shorter timescales via horizontal transfer and recombination (61), and drive
369 polymorphism in spectra across natural bacterial isolates (60, 62). We predict multiple cascading
370 effects of shifts in mutation spectra, including a reduction in the waiting time for beneficial
371 mutations, decreased likelihood of mutational meltdown under genetic drift, and distinct genetic
372 pathways of adaptation. We hope that future work will test these predictions.
373
374 **METHODS SUMMARY**
375
376 Here, we provide a summary of the methods important to understand our study. Details are given
377 in Supplementary Materials and Methods.
378
379 **Bacterial strains and mutation accumulation (MA) experiments**
380 We obtained the wild-type (WT) *E. coli* K-12 MG1655 strain and mutator strains (Δ*mutY*, Δ*ung* and
381 Δ*mutM* in *E. coli* K-12 BW25113) from the Coli Genetic Stock Centre (CGSC, Yale University). We
382 moved the Δ*mutY*, Δ*ung* and Δ*mutM* loci into the WT strain using P1-phage transduction and
383 confirmed the knockout using PCR and whole genome sequencing. To test whether genetic

384 background alters the fitness effects of single mutations observed during mutation accumulation
385 (MA), we deleted the *mutY* locus from 19 evolved WT MA lines using P1-phage transduction.
386
387 We founded WT, Δ*mutY*, Δ*ung* and Δ*mutM* MA lines from single colonies, and propagated them
388 through daily single-colony bottlenecks on LB agar for 8250, 330, 4400 and 5775 generations
389 respectively. The MA protocol minimizes the effect of selection, allowing us to sample a wide range
390 of mutations largely independent of their fitness consequences.
391
392 **Whole-genome sequencing to identify single mutations and determine mutation spectra**
393 We sequenced individual colonies from MA experiments to identify all clones carrying only a single
394 mutation relative to the WT or *ΔmutY* ancestor, using the Illumina HiSeq 2500 platform. For each
395 sample, we aligned quality-filtered reads to the NCBI reference *E. coli* K-12 MG1655 genome
396 (RefSeq accession ID GCA_000005845.2) and generated a list of base-pair substitutions and short
397 indels (<10bp). We calculated mutational biases as the fraction of each class of mutations
398 observed in our evolved strains (Table S3).
399
400 **Constructing single-mutation DFEs**
401 We measured growth rates of all evolved MA isolates with single mutations and their respective
402 ancestors in 16 different environments, and estimated maximum growth rate as a proxy of fitness.
403 For each isolate, we used the average growth rate of three technical replicates to calculate the
404 fitness effect (*s*) as (growth rate of evolved isolate/growth rate of ancestor) – 1. We used *s* values
405 of mutations to construct strain- and environment-specific distributions of fitness effects (DFE).
406 Although selection is minimized in MA experiments, it is not entirely avoided. We corrected both
407 WT and mutator DFEs for the effect of such selection as described recently (32), for each
408 environment. Calculations are shown in the Supplementary Data file.
409
410 **Estimating genetic load, beneficial mutation supply, and pleiotropy**
411 We used the mutation rate and f_b (estimated via the DFE) of WT and mutator in each environment
412 to estimate the deleterious load and supply of beneficial mutations, as described earlier (33)

413 (Tables S4 and S5). To predict the impact of the strain-specific DFEs on adaptation in new habitats,
414 we estimated the incidence of antagonistic and synergistic pleiotropy among new mutations
415 sampled by each strain. Results for WT *E. coli* in some environments were previously reported
416 (30). We similarly estimated pleiotropy of the 79 single mutations that arose in the mutator (Δ*mutY*)
417 background, and compared the incidence of pleiotropy across strains.
418
419 **Simulations to test the effect of mutation spectrum changes**
420 We used an established evolutionary model to test whether and to what extent changes in mutation
421 spectra are generally expected to affect the DFE. Following Stoltzfus (63), we simulated adaptive
422 walks on the NK fitness landscape (48), modelling sequences composed of strings of four bases
423 (A, C, G, T), allowing mutations to be classified as transitions or transversions, GC→AT or AT→GC,
424 and so on. In an NK fitness landscape, each locus in the sequence is randomly assigned K
425 neighbours from among all loci in the model. The fitness contribution of locus i (ω_i) then depends
426 on the state of that locus and the state of its neighbours. For computational efficiency we initially
427 simulated adaptive walks (strong-selection weak-mutation regime). At various times during the
428 adaptive walk, we generated a DFE by randomly sampling new mutations from the set of available
429 single-step mutations and estimated key parameters such as f_b.
430
431 Next, we relaxed a number of assumptions to test the generality of the simulation results. We
432 investigated higher degrees of epistasis by varying both N and K. We also simulated full
433 populations, in which large numbers of mutations simultaneously segregate, and deleterious
434 mutations can fix. Finally, we implemented a codon-based model in which nucleotide sequences
435 evolved as described above, but fitness was defined by an NK fitness landscape based on amino
436 acid sequence.
437
438 **Inferring past evolutionary changes in mutation spectra**
439 We used data from mutation accumulation studies with *E. coli* to obtain the predicted effects of the
440 loss of 11 genes encoding DNA repair enzymes on the Tv bias and GC→AT bias (Table S12). To
441 determine the evolutionary history of these genes, we detected orthologues and mapped predicted

gain and loss events for each gene across the bacterial phylogeny, as described previously (49). We used the inferred state of all enzymes at every node in the tree (including the eubacterial ancestor and the extant taxa) to estimate the Tv and GC→AT bias at each node, relative to WT *E. coli*. For all lineages in the tree, we traced the change in bias over time, up to the extant taxon and used these data to calculate the observed number and direction of changes in bias in each lineage, categorising them as “no change”, “single change”, “reinforcement” and “reversal” (Fig. S14A). To derive expected changes in bias based on chance, we ran forward simulations on the transition rate matrices (describing inferred rates of enzyme state transitions) and used the number and direction of mutation bias changes in each simulation to calculate the average proportion of lineages showing a given number of reversals (or other changes in mutation bias) expected by chance (Fig. S14B).

Acknowledgements

We thank Shyamsunder Buddh, Brian Charlesworth, Deborah Charlesworth, Joachim Krug, Krushnamegh Kunte, Saurabh Mahajan, Christopher Marx, and Mukund Thattai for discussion; Joshua Miranda for assistance with MA experiments; and the NGS facility at the Bangalore Life Sciences Cluster. **Funding:** We acknowledge funding and support from the National Centre for Biological Sciences (NCBS-TIFR), the Council for Scientific and Industrial Research India (Senior Research Fellowship to MS), the University Grants Commission of India (Senior Research Fellowship to GDD), the Department of Science and Technology India (KVPY Fellowship to BAB), the Natural Sciences and Engineering Research Council of Canada (LMW), and the Wellcome Trust (GDD is supported by grant 210585/B/18/Z to Robert B. Russell; and DBT/Wellcome Trust India Alliance grant IA/I/17/1/503091 to DA). We also thank the International Centre for Theoretical Sciences (ICTS) for supporting the Bangalore School on Population Genetics and Evolution (code: ICTS/popgen2020/01), where this collaboration was initiated. **Competing interests:** Authors declare no competing interests. **Author contributions:** MS designed and conducted experiments, analysed data, and drafted the manuscript. GDD designed and conducted phylogenetic analyses. BAB conducted experiments and analysed data. LMW obtained funding, designed and conducted simulation analyses, and drafted the manuscript. DA conceived and designed experiments and

phylogenetic analyses, analysed data, obtained funding, and wrote the manuscript. **Data and materials availability:** All data used for experimental and phylogenetic analysis are available as Supplementary Information files. Code for simulations and phylogenetic analysis is available on Github (https://github.com/lmwahl/MutationSpectrum and https://github.com/gauravdiwan89/dfe_ms_phylo_analysis).

Figure 1. Mutator DFEs have a larger fraction of beneficial mutations than WT. Stacked bar plots show the observed proportion of beneficial (f_b), deleterious and neutral mutations in WT and mutator (Mut). Average values across environments are given in the key; asterisks indicate significant differences between WT and mutator f_b, colored to show the strain with higher f_b (Table S2).

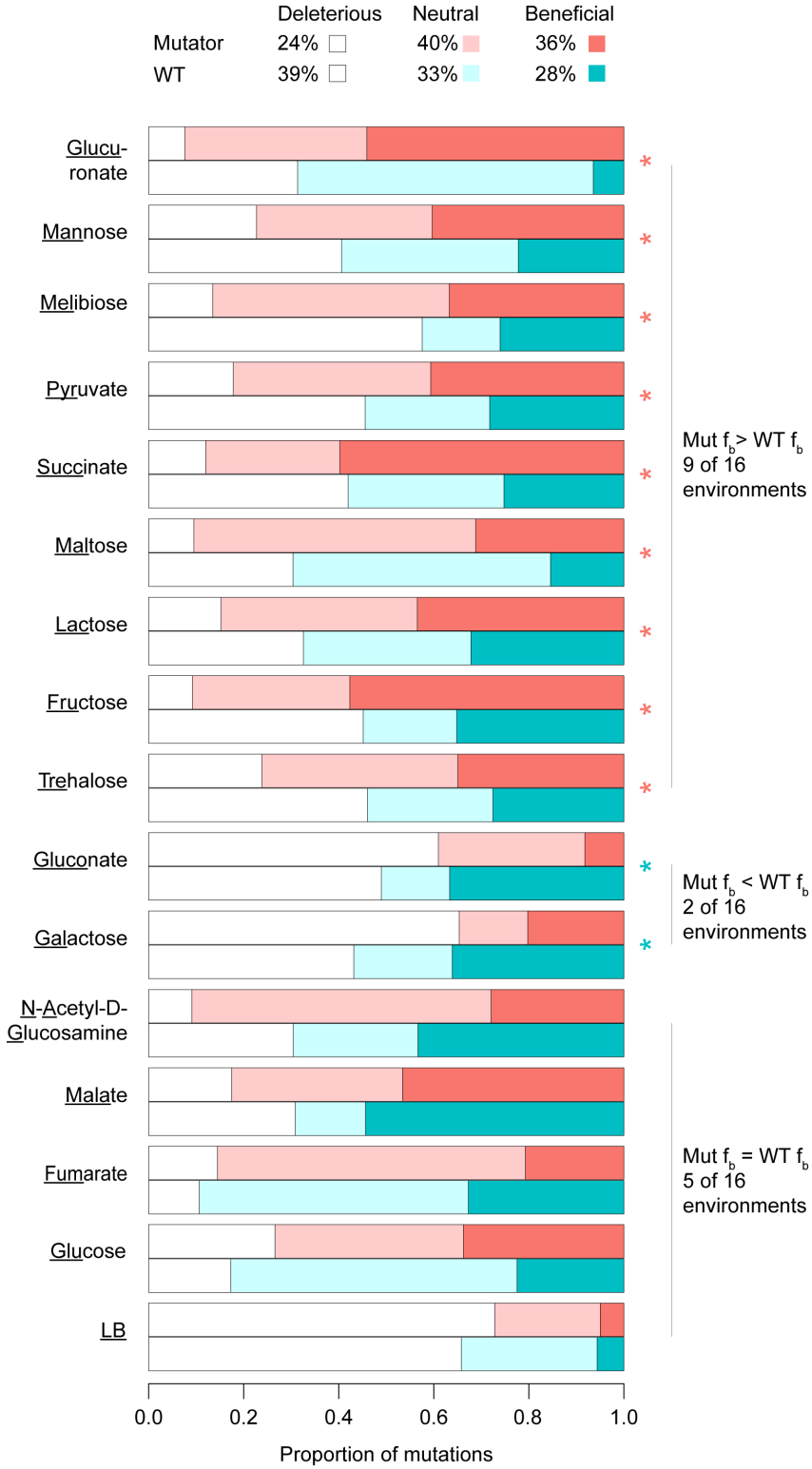

Figure 2. Beneficial-shifted DFE alters pleiotropic effects. (A) Schematic showing possible pleiotropic effects of mutations in two environments (W: relative fitness). (B–E) Median proportions of pleiotropic fitness effects (across 15 focal environments, excluding LB; also see Fig. S2C–F) of mutations in WT and mutator, and WT DFE artificially shifted towards either beneficial or deleterious mutations. Schematics indicate global DFEs (WT=cyan, mutator=pink, WT-shifted=light blue); black lines: relative fitness = 1. (F) Pleiotropic effects of mutations across multiple environments. Frequency distributions show the proportion of mutations with consistent fitness effects (beneficial or deleterious) in a given number of environments. Black lines indicate medians.

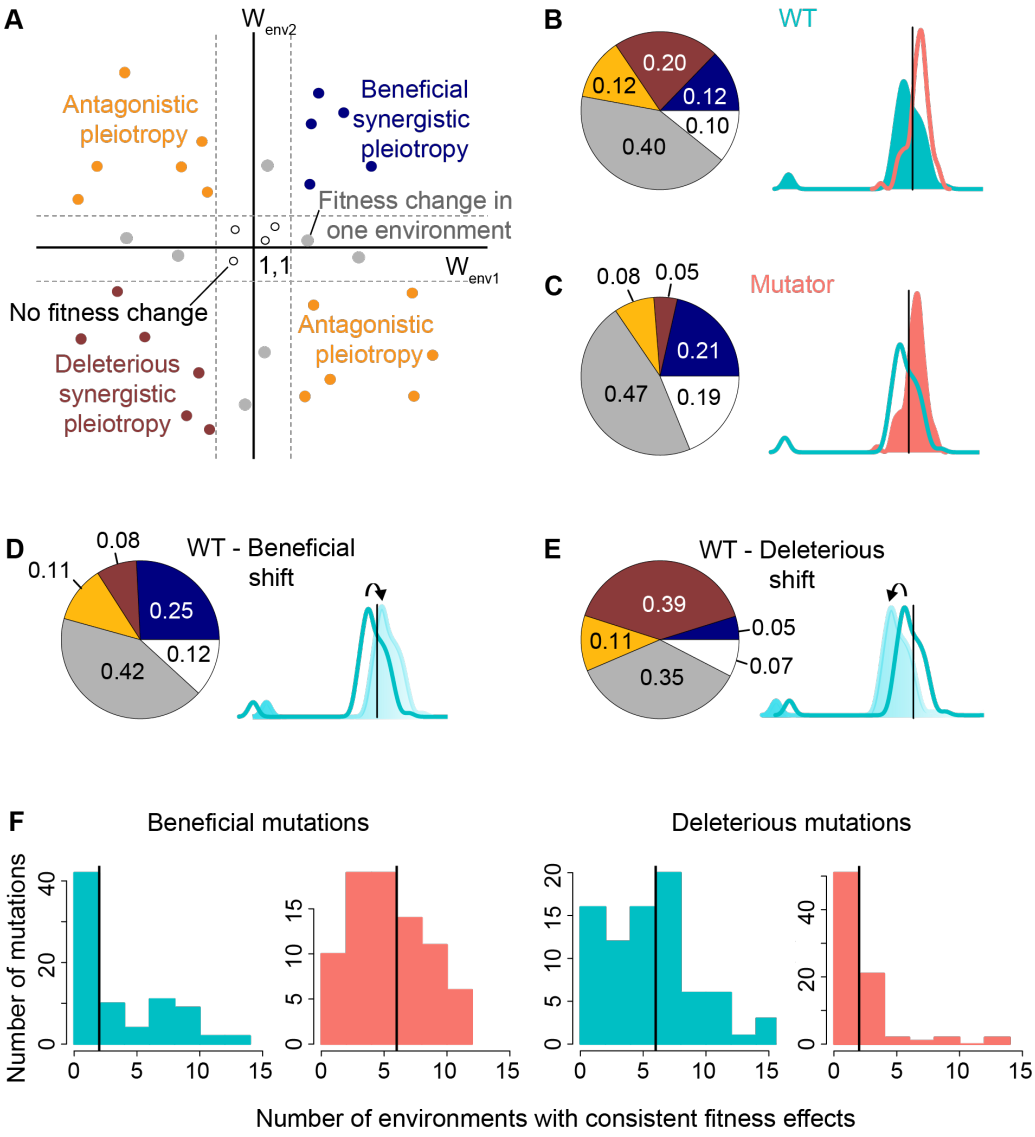

Figure 3. Differences in WT and mutator DFEs are best explained by differences in mutation spectra. (A) Growth rate of WT and mutator ancestors (n=12–24/strain/environment). Asterisks: significant differences between strains (Table S7). (B) Pairwise differences in the fitness effects of 19 mutations across genetic backgrounds (Mutator – WT); asterisks: significant difference from zero (black dotted line; Table S8). (C) Observed mutation biases in WT and mutator MA lines (including those with multiple mutations); the number of mutations of each type is noted. Asterisks: significant differences in proportions across strains; dashed line: no bias (Tv bias = 0.67, GC→AT bias = 0.5) (Table S3). (D–E) Fitness effects of different mutation classes, for MA-evolved isolates carrying single mutations. Boxplots (colored by strain and mutation class) show median, quartiles and range of relative fitness effects of mutations (open diamonds: outliers). Each boxplot was constructed with n x 16 data points (n = number of mutations, shown below each plot; pooled effects from 16 environments). Black horizontal lines: fitness impact = 0. Asterisks: significant differences across mutation classes (ANOVA output, Table S9; for imbalanced sample sizes, permutation tests as described for Fig. S4); nd: not determined.

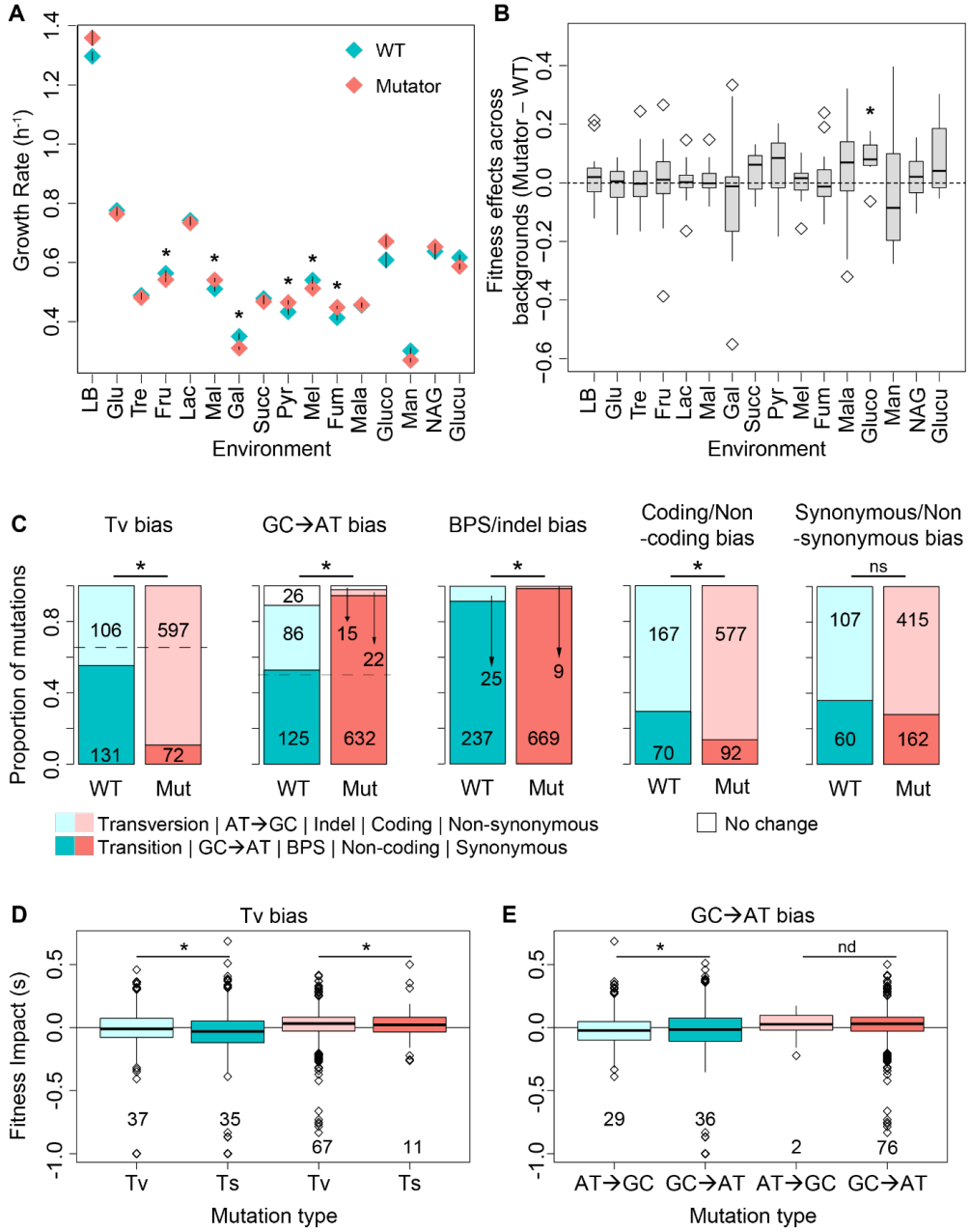

Figure 4. Simulations show a general benefit of reversing mutation spectra. (A) Change in mean population fitness, fraction of beneficial and deleterious mutations (f_b and f_d), and mean magnitude of beneficial and deleterious effects (s_b and s_d) over the course of adaptive walks of a WT ancestor. (B) Impact of altering the WT mutation bias on f_b at different points along the adaptive walk (Tv bias = Tv/(Ts+Tv) mutations; grey dashed line: WT bias), as a function of the new mutation bias (shifted Tv bias). Line color: WT f_b at a given time; steeper lines (lighter colors): later evolutionary time, better adapted WT. (C–D) Results as in (A–B) but for simulated populations of 100,000 individuals evolving for up to 100,000 generations with a mutation rate of 10^{-4} per genome per generation; the mean number of segregating genotypes in each generation was 77.8. (E–F) Impact of introducing a mutation bias in an unbiased ancestor ("anc"), as a function of the new bias (shifted Tv or GC→AT bias). Panels show the results of simulations identical to those described in panel B, but starting with an unbiased ancestor.

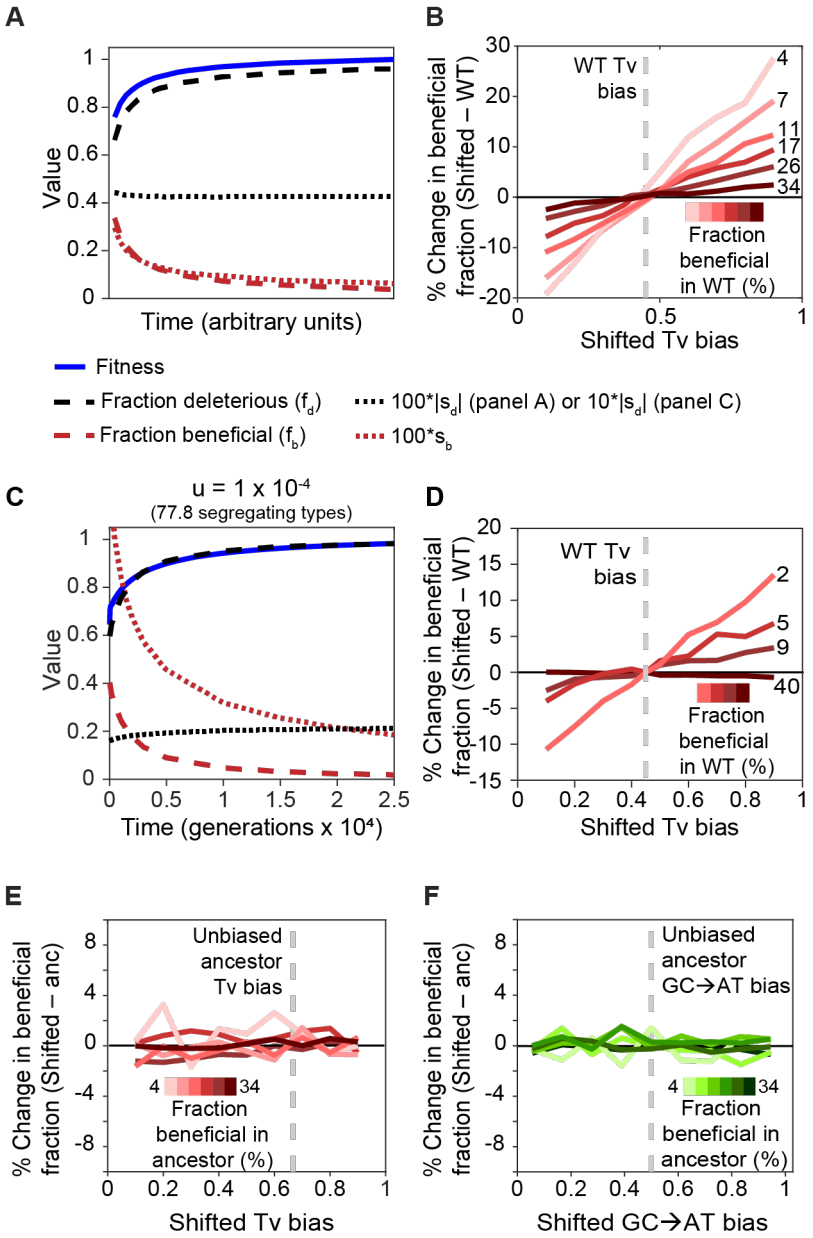

Figure 5. Phylogenetic analysis shows frequent evolutionary transitions in DNA repair genes and reversals in mutation spectra. (A) Patterns of gene presence/absence in extant taxa, used to map evolutionary transitions in DNA repair genes on the bacterial phylogeny (total transitions are shown in the key), and infer the magnitude of Tv and GC→AT biases relative to WT *E. coli* in extant taxa (heatmaps) based on experimental data from *E. coli* (Table S12). (B) Inferred trajectories of relative mutational biases across 1093 lineages (C) Observed number of lineages showing spectrum shifts due to successive evolutionary transitions in repair enzymes (% values calculated as fraction across all lineages; blue=observed; black=expected values, mean of 10,000 stochastic forward simulations, Fig. S14 C–D).

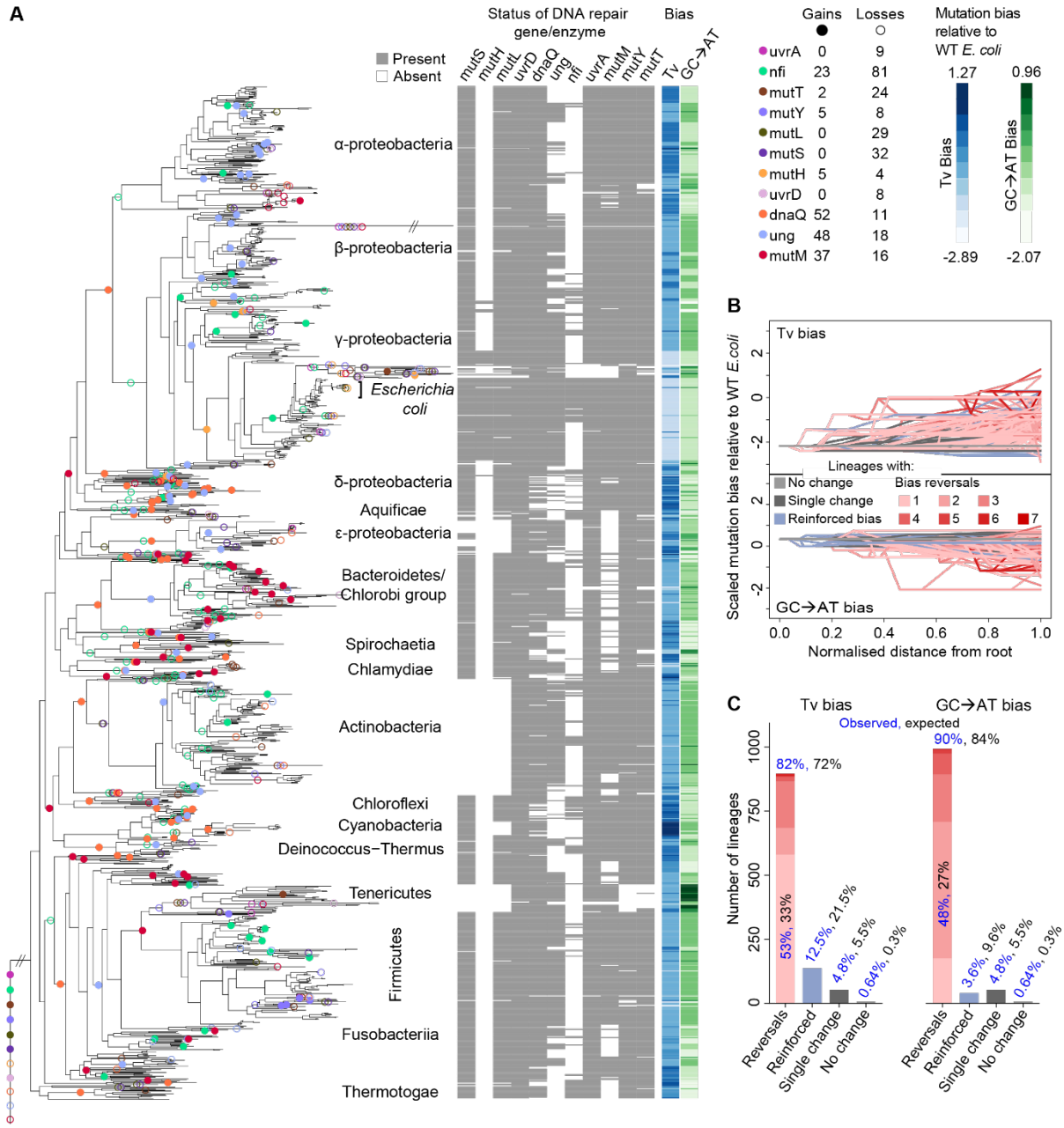

References

1. D. Agashe, N. Shankar, The evolution of bacterial DNA base composition. *Journal of Experimental Zoology Part B: Molecular and Developmental Evolution* 322, 517–528 (2014).
2. H. Long, *et al.*, Evolutionary determinants of genome-wide nucleotide composition. *Nature Ecology & Evolution* 48, 582 (2018).
3. J. Bohlin, O. Brynildsrud, T. Vesth, E. Skjerve, D. W. Ussery, Amino acid usage is asymmetrically biased in AT-and GC-rich microbial genomes. *PLoS ONE* 8, e69878 (2013).
4. A. Couce, *et al.*, Mutator genomes decay, despite sustained fitness gains, in a long-term experiment with bacteria. *Proceedings of the National Academy of Sciences of the United States of America* 259, 201705887–10 (2017).
5. A. Stoltzfus, L. Y. Yampolsky, Climbing Mount probable: Mutation as a cause of nonrandomness in evolution. *Journal of Heredity* 100, 637–647 (2009).
6. M. A. Streisfeld, M. D. Rausher, Population genetics, pleiotropy, and the preferential fixation of mutations during adaptive evolution. *Evolution* 65, 629–642 (2010).
7. D. R. Rokyta, P. Joyce, S. B. Caudle, H. A. Wichman, An empirical test of the mutational landscape model of adaptation using a single-stranded DNA virus. *Nature Genetics* 37, 441–444 (2005).
8. K. Gomez, J. Bertram, J. Masel, Mutation bias can shape adaptation in large asexual populations experiencing clonal interference. *Proc Royal Soc B* 287, 20201503 (2020).
9. A. V. Cano, J. L. Payne, Mutation bias interacts with composition bias to influence adaptive evolution. *Plos Comput Biol* 16, e1008296 (2020).
10. A. Stoltzfus, D. M. McCandlish, Mutational biases influence parallel adaptation. *Molecular Biology and Evolution* 34, 2163–2172 (2017).
11. J. F. Storz, *et al.*, The role of mutation bias in adaptive molecular evolution: insights from convergent changes in protein function. *Philosophical Transactions of the Royal Society B: Biological Sciences* 374, 20180238–10 (2019).
12. A. V. Cano, H. Rozhoňová, A. Stoltzfus, D. M. McCandlish, J. L. Payne, Mutation bias shapes the spectrum of adaptive substitutions. *Proc National Acad Sci* 119, e2119720119 (2022).
13. A. Couce, J. R. Guelfo, J. Blázquez, Mutational spectrum drives the rise of mutator bacteria. *PLoS Genetics* 9, e1003167 (2013).
14. J. L. Payne, *et al.*, Transition bias influences the evolution of antibiotic resistance in Mycobacterium tuberculosis. *PLoS Biology* 17, e3000265-23 (2019).
15. A. Bachar, *et al.*, Point mutations in topoisomerase I alter the mutation spectrum in E. coli and impact the emergence of drug resistance genotypes. *Nucleic Acids Research* 48, 761–769 (2019).
16. S. M. Leighow, C. Liu, H. Inam, B. Zhao, J. R. Pritchard, Multi-scale predictions of drug resistance epidemiology identify design principles for rational drug design. *Cell Reports* 30, 3951-3963.e4 (2020).
17. P. L. Foster, H. Lee, E. Popodi, J. P. Townes, H. Tang, Determinants of spontaneous mutation in the bacterium Escherichia coli as revealed by whole-genome sequencing. *Proceedings of the National Academy of Sciences of the United States of America*, 201512136–10 (2015).
18. Y. Raynes, P. D. Sniegowski, Experimental evolution and the dynamics of genomic mutation rate modifiers. *Heredity* 113, 375–380 (2014).
19. R. P. Maharjan, T. Ferenci, A shifting mutational landscape in 6 nutritional states: Stress-induced mutagenesis as a series of distinct stress input–mutation output relationships. *PLoS Biology* 15, e2001477-22 (2017).
20. S. Shewaramani, *et al.*, Anaerobically grown Escherichia coli has an enhanced mutation rate and distinct mutational spectra. *PLoS Genetics* 13, e1006570-22 (2017).
21. P. Jiang, *et al.*, A modified fluctuation assay reveals a natural mutator phenotype that drives mutation spectrum variation within Saccharomyces cerevisiae. *Elife* 10, e68285 (2021).
22. E. López-Cortegano, *et al.*, De novo mutation rate variation and its determinants in Chlamydomonas. *Mol Biol Evol* 38, msab140- (2021).
23. T. Ferenci, Irregularities in genetic variation and mutation rates with environmental stresses. *Environmental Microbiology* 21, 3979–3988 (2019).
24. V. Katju, U. Bergthorsson, Old trade, new tricks: Insights into the spontaneous mutation process from the partnering of classical mutation accumulation experiments with high-throughput genomic approaches. *Genome Biology and Evolution* 11, 136–165 (2018).
25. L. Y. Yampolsky, A. Stoltzfus, Bias in the introduction of variation as an orienting factor in evolution. *Evolution and Development* 3, 73–83 (2001).
26. D. Agashe, The road not taken: Could stress-specific mutations lead to different evolutionary paths? *PLoS Biology* 15, e2002862-5 (2017).

27. A. Stoltzfus, R. W. Norris, On the causes of evolutionary transition:transversion bias. *Molecular Biology and Evolution* 33, 595–602 (2016).
28. D. M. Lyons, A. S. Lauring, Evidence for the Selective Basis of Transition-to-Transversion Substitution Bias in Two RNA Viruses. *Mol Biol Evol* 34, 3205–3215 (2017).
29. Z. Zou, J. Zhang, Are nonsynonymous transversions generally more deleterious than nonsynonymous transitions? *Mol Biol Evol* 38, msaa200- (2020).
30. M. Sane, J. J. Miranda, D. Agashe, Antagonistic pleiotropy for carbon use is rare in new mutations. *Evolution* 72, 2202–2213 (2018).
31. D.-E. Chang, *et al.*, Carbon nutrition of Escherichia coli in the mouse intestine. *P Natl Acad Sci Usa* 101, 7427–7432 (2004).
32. L. M. Wahl, D. Agashe, Selection bias in mutation accumulation. *Evolution* 76, 528–540 (2022).
33. S. Wielgoss, *et al.*, Mutation rate dynamics in a bacterial population reflect tension between adaptation and genetic load. *Proceedings of the National Academy of Sciences* 110, 222–227 (2013).
34. A. Eyre-Walker, P. D. Keightley, The distribution of fitness effects of new mutations. *Nature Reviews Genetics* 8, 610–618 (2007).
35. M. Weng, *et al.*, Fitness effects of mutation in natural populations of Arabidopsis thaliana reveal a complex influence of local adaptation. *Evolution* (2020) https:/doi.org/10.1111/evo.14152.
36. C. Zeyl, J. A. DeVisser, Estimates of the rate and distribution of fitness effects of spontaneous mutation in Saccharomyces cerevisiae. *Genetics* 157, 53–61 (2001).
37. D. W. Hall, S. B. Joseph, A High Frequency of Beneficial Mutations Across Multiple Fitness Components in Saccharomyces cerevisiae. *Genetics* 185, 1397–1409 (2010).
38. S. B. Joseph, D. W. Hall, Spontaneous Mutations in Diploid Saccharomyces cerevisiae More Beneficial Than Expected. *Genetics* 168, 1817–1825 (2004).
39. W. J. Dickinson, Synergistic Fitness Interactions and a High Frequency of Beneficial Changes Among Mutations Accumulated Under Relaxed Selection in Saccharomyces cerevisiae. *Genetics* 178, 1571–1578 (2008).
40. L. Perfeito, L. Fernandes, C. Mota, I. Gordo, Adaptive mutations in bacteria: high rate and small effects. *Science* 317, 813–815 (2007).
41. C. Kozela, M. O. Johnston, Effect of Salt Stress on Mutation and Genetic Architecture for Fitness Components in Saccharomyces cerevisiae. *G3 Genes Genomes Genetics* 10, g3.401593.2020 (2020).
42. R. G. Shaw, F. H. Shaw, C. Geyer, What fraction of mutations reduces fitness? A reply to Keightley and Lynch. *Evolution* 57, 686–689 (2003).
43. J. W. Thatcher, J. M. Shaw, W. J. Dickinson, Marginal fitness contributions of nonessential genes in yeast. *Proc National Acad Sci* 95, 253–257 (1998).
44. M. Imhof, C. Schlötterer, Fitness effects of advantageous mutations in evolving Escherichia coli populations. *Proc National Acad Sci* 98, 1113–1117 (2001).
45. F. H. Shaw, C. J. Geyer, R. G. Shaw, A comprehensive model of mutations affecting fitness and inferences for Arabidopsis thaliana. *Evolution* 56, 453–463 (2002).
46. R. G. Shaw, D. L. Byers, E. Darmo, Spontaneous Mutational Effects on Reproductive Traits of Arabidopsis thaliana. *Genetics* 155, 369–378 (2000).
47. H. A. Orr, The population genetics of adaptation: The distribution of factors fixed during adaptive evolution. *Evolution* 52, 935–949 (1998).
48. C. A. Macken, A. S. Perelson, Protein evolution on rugged landscapes. *Proceedings of the National Academy of Sciences of the United States of America* 86, 6191–6195 (1989).
49. G. D. Diwan, D. Agashe, Wobbling Forth and Drifting Back: The Evolutionary History and Impact of Bacterial tRNA Modifications. *Mol Biol Evol* 35, 2046–2059 (2018).
50. J. A. Eisen, P. C. Hanawalt, A phylogenomic study of DNA repair genes, proteins, and processes. *Mutation research* 435, 171–213 (1999).
51. J. B. Losos, Seeing the Forest for the Trees: The Limitations of Phylogenies in Comparative Biology: (American Society of Naturalists Address). *Am Nat* 177, 709–727 (2011).
52. M. Sharda, A. Badrinarayanan, A. S. N. Seshasayee, Evolutionary and Comparative analysis of bacterial Non-Homologous End Joining Repair. *Genome Biol Evol* 12, evaa223- (2020).
53. M. A. Phillips, J. L. Steenwyk, X.-X. Shen, A. Rokas, Examination of gene loss in the DNA mismatch repair pathway and its mutational consequences in a fungal phylum. *Genome Biol Evol*, evab219- (2021).
54. K. Jain, A. James, Fixation probability of a nonmutator in a large population of asexual mutators. *Journal of Theoretical Biology* 433, 85–93 (2017).

55. J. A. G., *et al.*, Diminishing Returns from Mutation Supply Rate in Asexual Populations. *Science* 283, 404–406 (1999).
56. O. Tenaillon, B. Toupance, H. L. Nagard, F. Taddei, B. Godelle, Mutators, population size, adaptive landscape and the adaptation of asexual populations of bacteria. *Genetics* 152, 485–493 (1999).
57. C. F. Gentile, S.-C. Yu, S. A. Serrano, P. J. Gerrish, P. D. Sniegowski, Competition between high- and higher-mutating strains of Escherichia coli. *Biology Letters* 7, 422–424 (2010).
58. A. Couce, O. Tenaillon, Mutation bias and GC content shape antimutator invasions. *Nature communications* 10, 3114–9 (2019).
59. L. Notley-McRobb, S. Seeto, T. Ferenci, Enrichment and elimination of mutY mutators in Escherichia coli populations. *Genetics* 162, 1055–1062 (2002).
60. I. Matic, *et al.*, Highly variable mutation rates in commensal and pathogenic Escherichia coli. *Science* 277, 1833–1834 (1997).
61. E. Denamur, *et al.*, Evolutionary implications of the frequent horizontal transfer of mismatch repair genes. *Cell* 103, 711–721 (2000).
62. J. E. LeClerc, B. Li, W. L. Payne, T. A. Cebula, High mutation frequencies among Escherichia coli and Salmonella pathogens. *Science* 274, 1208–1211 (1996).
63. A. Stoltzfus, Mutation-biased adaptation in a protein NK model. *Molecular Biology and Evolution* 23, 1852–1862 (2006).